Load Pull-Driven Behavioral Modelling of Microwave Switches for the Design of Tunable Reflective Terminations

Seyed U. Ghozati[#1], Roberto Quaglia[#], Ehsan Azad [#$2], Jeff Powell [*3], Paul Tasker [#], Steve Cripps [#]

[#]Centre for High-Frequency Engineering, Cardiff University, UK

[$]Compound Semiconductor Application Catapult, UK

[*]Skyarna Ltd, UK

[1]GhozatiSU@Cardiff.ac.uk, [2]Ehsan.Azad@CSA.Catapult.org.uk, [3]Jeff.powell@skyarna.com

***Abstract*— Recent advances in RFPA design make extensive use of active load modulation techniques. These architectures can be made more effective by the insertion of electronically tuneable reactive elements. This work describes the measurement and modeling of microwave switches aimed at this application. Active open-loop load-pull measurements were performed on microwave switches with different biasing voltages and power levels. Using load-pull measurement data, the devices are modeled based on Cardiff behavioral model's mathematics expressing good accuracy in reproducing the switch response in the linear and compression regions.**

***Keywords*— Behavioral modelling, gallium nitride, load pull measurements, microwave switches.**

I. Introduction

Solid-State microwave switches (MSs), such as those based on FETs and PIN diodes, have become highly sought within all communication systems due to their compact size, enhanced durability, and compatibility with MMIC designs [1]. Benefitting from emerging compound semiconductor (CS) technologies, such as gallium nitride (GaN), performance of MSs further enhanced with reduced insertion loss, higher isolation, greater power handling capabilities, improved linearity, and lower DC power consumption.

Traditionally, MSs have been utilized solely for enabling signal propagation or blockage along specific pathways. However, they are increasingly being employed in the realization of switch-type phase shifters (STPS) [2-3], microwave attenuators [4-5], and the synthesis of variable impedances (e.g., voltage/current-dependent RF resistors, or within automatic calibration kits) [6-8]. This paper draws motivation from the latter, where the control of the reflection coefficient can be achieved through voltage manipulation of FET-based devices switching between various inductive and capacitive loads, as in Fig. 1.

An application example that employs MSs in this mode is the Orthogonal Load Modulated Balanced Amplifier (OLMBA) [9-10], a variant of the Load Modulated Balanced Amplifier (LMBA) [11]. The LMBA modulates the load dynamically by injecting a signal called the Control Signal Power (CSP) into the output isolated port of a balanced amplifier architecture. In contrast, the OLMBA utilizes CSP at the input and a tunable reactive termination at the output, as shown in Fig. 1, to fully exploit the degrees of freedom of load modulation and reconfigurability. Previous implementations of the tunable termination have used Si-based switches [10], limiting their utility to relatively low average power. Therefore, GaN-based switches are interesting for realizing the tunable reflective termination, as they offer higher power handling capabilities. This tunable termination can be implemented with one or multiple switches, arranged in series or shunt connection, and a few reactive components, as depicted in Fig. 1.

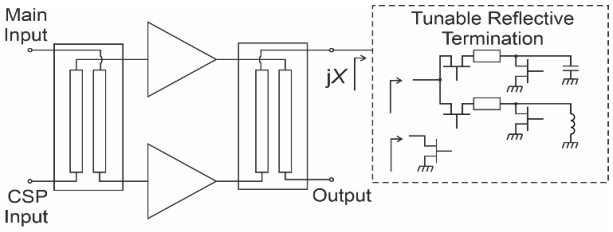

Fig. 1. Schematic of OLMBA with Tunable Reflective Termination where different microwave switches configurations can be employed.

This paper employs load-pull characterization to examine the performance of switches and develop a model under various loading conditions. This methodology enables the emulation of both series and shunt connections and facilitates the measurement of the response of the switch when it is introduced to a highly reflective impedance environment of tunable terminations.

II. Standard Measurements

In preparation for designing a tunable termination network and identifying a narrower set of active devices, it is imperative to conduct standard measurements to determine the performance of devices in the frequency domain in terms of insertion loss and isolation. This is accomplished by

identifying the most appropriate ON and OFF control voltages as well as power handling determination through a 50 Ohm power sweep.

A group of switches based on high electron mobility transistors (HEMTs) with 150 nm gate-length and GaN on SiC technology have been analyzed. These switches were sourced from WIN Semiconductors Corp. and are constructed with a symmetric device layout, with variations in the number of gate fingers (3, 5, 7, and 9) and two distinct gate widths (50 µm and 100 µm). A series configuration with the gate grounded through an isolation resistor of 4.5 kΩ enables the device to be characterized on the wafer via the GSG microstrip launchers. External bias tees for the drain and source are connected to the same positive control voltage (refer to Fig. 2).

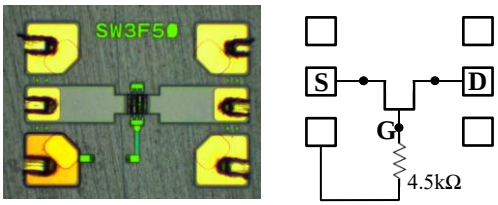

Fig. 2. Schematic and picture of the switch configuration used for testing. The depicted switch is a 3-finger with 50um gate width.

A. S-Parameters

S-parameter measurements were performed on-wafer up to 25 GHz using a TRM calibration with ad-hoc calibration standards to align the reference planes to the device level. Various voltages were investigated and led to determining 0 V and 20 V as optimum voltages, for OFF and ON conditions, respectively. As it can be realised from the measurement results illustrated in Fig. 3, the smallest device (3F50) has the best isolation and worst insertion loss, while the opposite occurs for the largest device size (9F100).

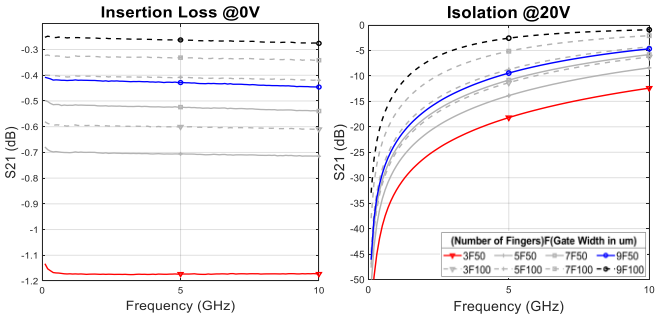

Fig. 3. Scattering parameter measurement results zoomed in to 0 to 10GHz for different device sizes. Insertion loss in ON mode (left) and isolation in OFF mode (right) vs. frequency. Device size expressed as (*number of fingers*)F(*gate width in um*).

B. 50 Ohm Power Sweeps

The 50 Ohm power sweeps offer scalar information on the compression behavior in terms of insertion loss (for the ON condition) and reflection coefficient magnitude (for the OFF condition). The selected devices, with periphery scaling of 1x (3F50), 3x (9F50) and 6x (9F100), are excited with CW single-tone signal at 3 GHz.

Fig.4 shows the results in ON and OFF condition. In ON condition, the smallest device (3F50) exhibits compression starting at approximately 20 dBm of input power. In contrast, the largest device (9F100) only displays 0.1 dB of compression at 40 dBm input power. Regarding the OFF condition, it is realized that the applied voltage, rather than the periphery, is the primary factor. A 20 V bias voltage demonstrates the highest power handling no matter of the size of the device, where the magnitude of the input reflection coefficient begins to decrease at around 35-38 dBm of input power for the devices under test.

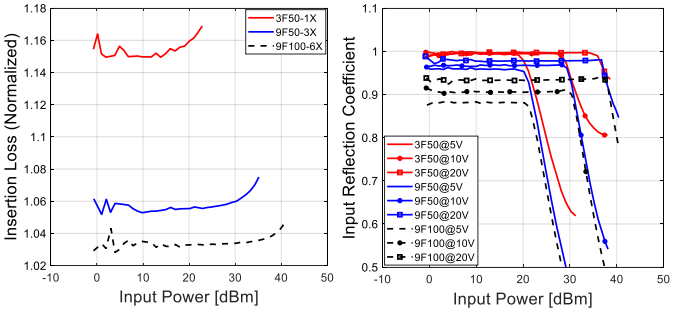

Fig. 4. 50 Ohm power sweep results at 3 GHz with CW excitation. The input power refers to the input reference plane of the switch. Insertion loss in ON mode (top); input reflection coefficient in OFF mode for different bias (bottom).

Fig. 5 illustrates, the evolution of input reflection coefficients on the Smith Chart as power increases in the OFF condition, indicating that larger devices are initially more capacitive and less reflective. Additionally, it reveals that a phase change occurs just before entering compression, and this information could not be captured with a scalar 50 Ohm measurement.

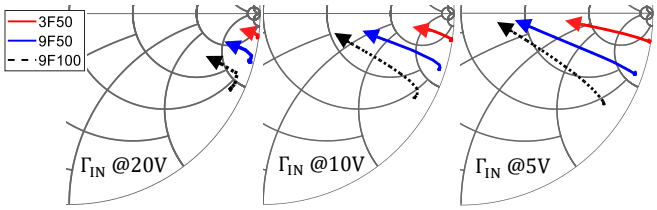

Fig. 5. Input reflection coefficient vs. input power for different device sizes in different bias cases for OFF condition, at 3 GHz.

III. Load Pull Measurements

The load-pull measurement system used in this study is an open-loop active system, as shown in Fig. 6. The calibrated waves are measured by a Rohde and Schwarz ZVA67 Vector Network Analyzer (VNA). The internal sources of the VNA are utilized to generate the input and load-pull signals, with the RF signals amplified by high-power driver amplifiers.

Figure 7. illustrates the load-pull measurement results for the 3F50 (top) and 9F100 (bottom) devices in both ON and OFF conditions at two different drive levels chosen by observing the 50 Ohm power sweep. The first power level is in the linear region (blue triangles) while the other is at 1dB compression (red triangles) of either insertion loss in the ON condition (left), or input reflection coefficient in the OFF condition (right). The black crosses represent the load tested.

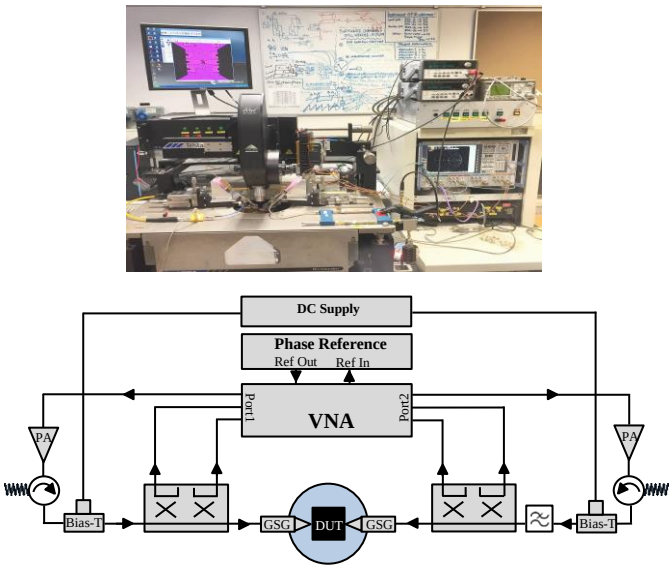

Fig. 6. Picture and block diagram of the active load pull setup.

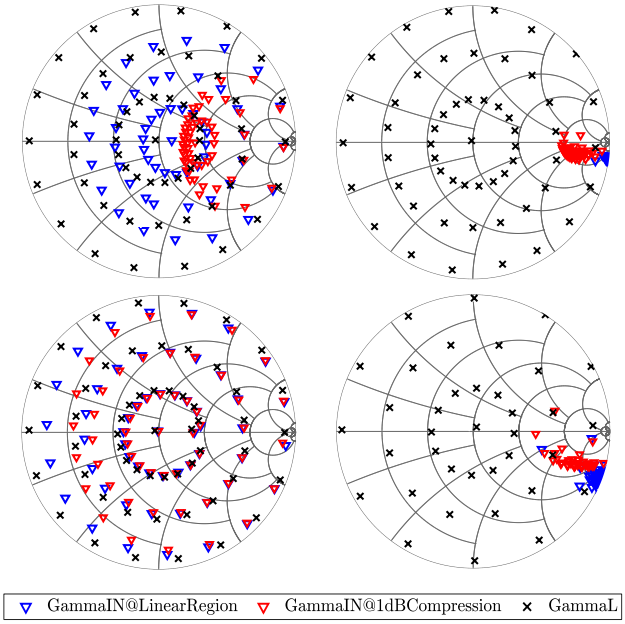

Fig. 7. Load pull measurement results at 3 GHz for the 3F50 switch (top) and the 9F100 switch (bottom), in ON (left) and OFF (right) conditions. Drive level: linear region (blue triangle) and 1 dB compression (red triangle).

In the ON condition, compression reduces the coverage of the Smith Chart, particularly from the left-hand side, due to the dominant parasitic being the ON resistance, which is magnified when a low impedance loads the switch. This effect is more substantial in compression, indicating that the main consequence of compression is an increase in the equivalent ON resistance in the switch. In the OFF condition, the input reflection coefficient is less dependent on the load due to isolation, but non-perfect isolation leads to a pulling of the input impedance, which becomes more extensive in compression when the isolation is compromised.

IV. Behavioral Modelling

The experimental findings have revealed that the switch's response under compression is complex, with combined phase and magnitude deviations from the linear response. The Cardiff behavioral model [12] can be utilized to incorporate the measured load-pull data into a CAD software environment. This model mathematically represents the nonlinear relationship between incident waves "A" and reflected waves "B" at the DUT plane:

$$B_{p,h} = \left(\angle A_{1,1}\right)^h \sum_{r=0}^{1} \sum_{n=n_{min}}^{n_{max}} K_{p,h,m,n} \left|A_{2,1}\right|^m \left(\frac{\angle A_{2,1}}{\angle A_{1,1}}\right)^n$$

$$\begin{cases} n_{min} = -\left(\dfrac{w-h}{2} - r\right) \\ n_{max} = h + \left(\dfrac{w-h}{2} - r\right) \\ m = |n| + 2r \end{cases}$$

In (1), "p" and "h" are port and harmonic index, respectively; "m" and "n" are $(A_{2,1})$ magnitude and phase exponents, while the magnitude indexing is represented by the term "r" which has a maximum value of "1." The model order "w" defines the complexity of the model. The model extraction process involves the identification of the coefficients "K" and can be easily performed with a least mean square algorithm.

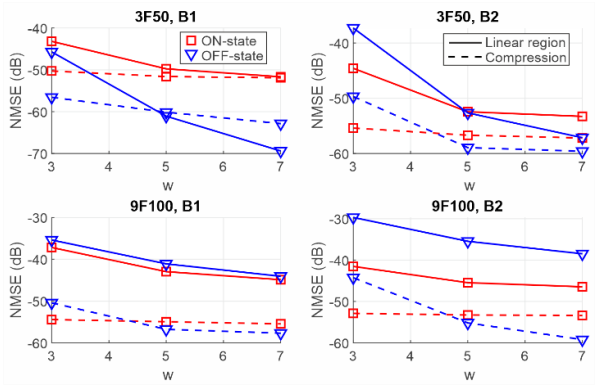

Fig. 8. NMSE vs. model order for modelling B1 and B2 in both ON and OFF conditions at different drive levels.

Since the Cardiff model has been used almost exclusively to model transistors in active mode, in the case of switch modeling, to determine the appropriate model complexity for the highest achievable model accuracy, the model complexity (w) of 3, 5, and 7 are calculated by means of Normalized Mean Square Error (NMSE), which is a figure of merit to calculate the overall deviation of the measurement and predicted data (modelled). The equation below illustrates the definition of NMSE.

$$NMSE = \frac{1}{N} \sum_i \frac{(P_i - M_i)^2}{\bar{P}\bar{M}}$$

$$\bar{P} = \frac{1}{N} \sum_i P_i$$

$$\bar{M} = \frac{1}{N} \sum_i M_i$$

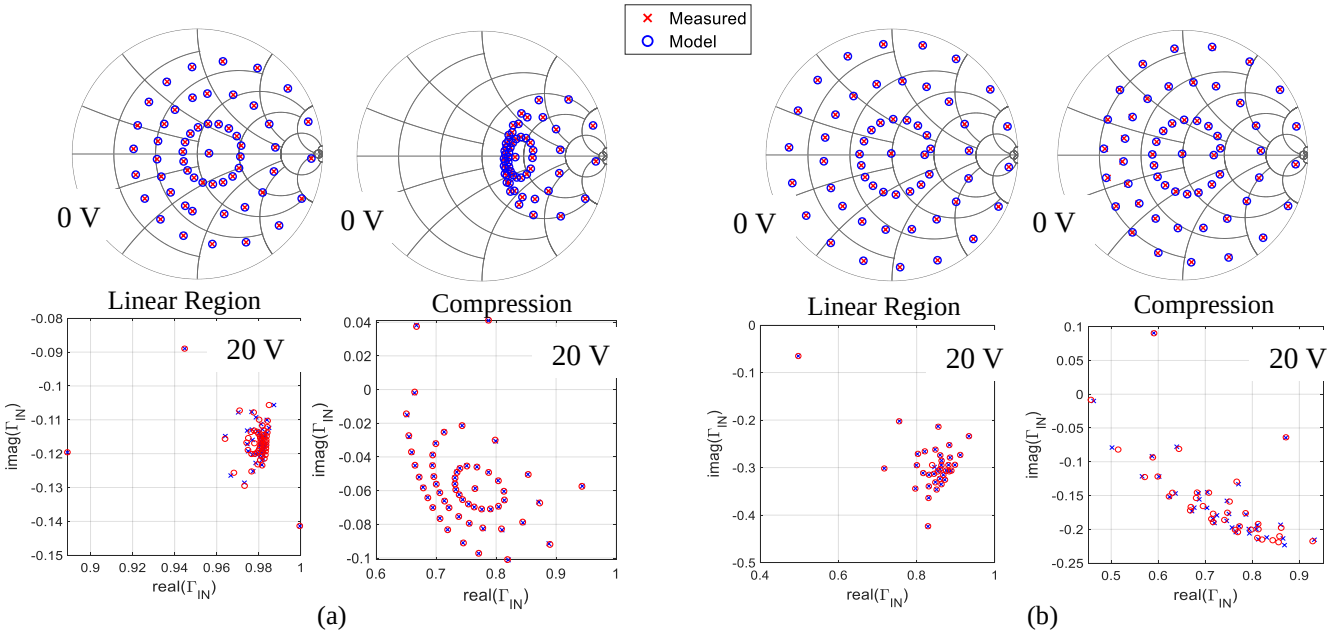

Fig. 9. Input reflection coefficient results for 3F50 (a) and 9F100 (b), measured (red cross) and model (blue circle) at ON mode (smith charts) and OFF mode (rectangle figures) in linear region (left figures) and 1 dB compression (right figures).

Where 'M' and 'P' represent the measured and predicted (or modelled) data, respectively. The letter 'N' represents the number of loads measured during the load-pull measurement. As it is depicted in Fig. 8, a model order of 5 can achieve outstanding accuracy on all interesting parameters.

In Fig. 9, the input reflection coefficient of the 3F50 and 9F100 devices in both linear and compression regions for ON and OFF conditions is compared between the modeled and measured results. The model order of $w = 5$ is used for all cases, demonstrating the model's capability to replicate the switch response in both states accurately.

V. Conclusion

Microwave switches can be used in various configurations to form a tunable termination capable of loading with high reflective loads. This study performed load-pull measurements and behavioral modeling to accurately capture the responses and reproduce the behavioral model of switches, which will be used in the CAD environment for further tunable termination network design work. Further work can be done measuring waveforms and obtaining a better understanding of weak non-linear response for using these switches in linear amplifier applications.

Acknowledgment

I acknowledge the support of WIN Semiconductors Corp. in providing the semiconductor devices used in this research.

References

[1] S. C. Bera, Microwave active devices and circuits for communication, Lecture Notes in Electrical Engineering, vol. 533. Ahmedabad, Gujarat, India: Springer, 2019, pp. 199–233.

[2] P. Gu and D. Zhao "A Ka-Band CMOS Switched-Type Phase Shifter with Low Gain Error" in IEEE International Conference on Integrated Circuits, Technologies and Applications (ICTA), 2021, National Mobile Communication Research Laboratory, Southeast University, Nanjing, China.

[3] Y. J. Liang et al., "A 19-GHz 5-Bit Switch-Type Phase Shifter Design Using Phase Compensation Techniques" in EEE International Symposium on Radio-Frequency Integration Technology (RFIT), 2021.

[4] Y. Tajima et al., "GaAs Monolithic Wideband (2-18 GHz) Variable Attenuators" in IEEE MTT-S International Microwave Symposium Digest, 1982.

[5] S. M. Daoud et al., "A Novel Wideband MMIC Voltage Controlled Attenuator with a Bandpass Filter Topology" in IEEE Transactions on Microwave Theory and Techniques, VOL. 54, NO. 6, 2006.

[6] F. Drillet et al., "RF Small and large signal characterization of a 3D integrated GaN/RF-SOI SPST switch" International Journal of Microwave and Wireless Technologies, Cambridge University Press, 2021.

[7] A. Bettidi et al., "High Power GaN-HEMT Microwave Switches for X-Band and Wideband Applications" in IEEE Radio Frequency Integrated Circuits Symposium, 2008.

[8] W. Ciccognani et al., "High Isolation Microstrip GaN-HEMT Single-FET Switch" published in Wiley InterScience, 2010.

[9] R. Quaglia and S. Cripps, "A Load Modulated Balanced Amplifier for Telecom Applications" in IEEE Transactions on Microwave Theory and Techniques, VOL. 66, NO. 3, 2018.

[10] R. Quaglia et al., "Mitigation of Load Mismatch Effects Using an Orthogonal Load Modulated Balanced Amplifier," in IEEE Transactions on Microwave Theory and Techniques, vol. 70, no. 6, pp. 3329-3341, June 2022.

[11] D. Shepphard et al., "An Efficient Broadband Reconfigurable Power Amplifier Using Active Load Modulation" in IEEE Microwave and Wireless Components Letters, VOL. 26, NO. 6, 2016.

[12] E. M. Azad et al., "New Formulation of Cardiff Behavioral Model Including DC Bias Voltage Dependence" in in IEEE Microwave and Wireless Components Letters, VOL. 32, NO. 6, June 2022.